



ELSEVIER

Contents lists available at SciVerse ScienceDirect

Measurement

journal homepage: www.elsevier.com/locate/measurement

3-D measurement and evaluation of surface texture produced by scraping process

Kuang-Chao Fan^{a,*}, Jingsyan Torng^b, Wenyuh Jywe^c, Rui-Chen Chou^a, Jyun-Kuan Ye^a

^a Department of Mechanical Engineering, National Taiwan University, Taiwan

^b Department of Mechanical Engineering, Nanya Institute of Technology, Chungli, Taiwan

^c Department of Automation Engineering, National Formosa University, Huwei, Taiwan

ARTICLE INFO

Article history:

Received 25 November 2010

Received in revised form 13 October 2011

Accepted 13 November 2011

Available online xxxx

Keywords:

Scraped surface

Surface quality parameter

Image measurement system

Laser focus probe system

3-D topography

ABSTRACT

The scraping process involves traditional manual work and is an important technique for producing flat bearing surfaces with lubricating grooves on a sliding surface. In order to meet the requirements of precision engineering, the scraped surface should have an equally distributed pattern with a required number of high points per unit area while retaining good flatness. In the machine tool manufacturer's workshop, however, the quality inspection of scraped surfaces still depends on human eyes. In this study, a 2-D evaluation system is first developed using image processing so that the peak points per area of square inch (PPI) and the percentage of points (POP) can be quantified as parameters. A vision-assisted laser focus probe system is then developed to measure the 3-D form of the scraped profiles. The laser probe is made of a DVD pickup head based on the astigmatic principle. Driven by an XY stage, the entire scraped profile can rapidly be scanned. The quality of the scraped surface can thus be interpreted in a more scientific manner. Based on the measured 3-D data, new evaluation methods are proposed for five parameters, namely the PPI, POP, height of points (HOP) or depth of surroundings (DOS), flatness, and oil retention volume. Experiments show that the 3-D system is consistent with the 2-D system. It not only reveals more surface quality parameters but also uncovers more characteristic surface phenomena than the 2-D image system.

© 2011 Elsevier Ltd. All rights reserved.

1. Introduction

The precision of a machine tool is crucial for the final dimensions of a workpiece. For heavy-duty machine tools, the guideway of each axis is in direct sliding contact with the moving carriage, rather than indirectly via a linear guideway mounted in between. The two contact surfaces must be carefully scraped to create a flat bearing profile with lubricating spots in various patterns. It is required that the relative motion of the two sliding surfaces is smooth under sufficient lubrication with oil. An important factor that influences the precision of the workpiece is the quality of the scraping process on the guideway surface.

The current scraping technique involves the initial application of a tinted (blue or red) paste to the contact surface of the guideway during assembly. Secondly, a stretch (or perfectly flat tool) is passed over areas highlighted by the tinted paste, allowing the engineer to see any areas that may not be even or level. The tinted marks representing high points are visible from the paste and represent the areas that need to be hand-scraped and properly fit to ensure geometric alignment of the machine tool. The scraping process requires highly experienced skill. A skilled craftsman must practice for a long time to acquire the hand- or power-scraping technique. This kind of work is extremely labor intensive. Nowadays, qualified scraping technicians are becoming fewer and fewer in the machine tool industry.

According to commonly accepted knowledge of the scraping technique, there are five parameters to evaluate

* Corresponding author. Tel.: +886 2 23620032.

E-mail address: fan@ntu.edu.tw (K.-C. Fan).

on the scraped surface [1]. The two most important parameters are the peak points per area of square inch (PPI) and the percentage of points (POP). This means that the surface must contain enough high points and a sufficient area to bear the load on the surface top. The indented portion is used to contain oil for lubrication. The current 2-D inspection method for these two parameters in the industry involves judging the tinted pattern distribution by eye. The other three parameters are the height of points (HOP) or depth of surroundings (DOS) to estimate oil containment, the shape of the cavity edge to avoid oil push-out and dirt push-in, and the flatness of the scraped surface to assure a smooth motion. These three parameters can only be judged by a 3-D view. However, none of the existing methods can provide this information.

Using computer vision to examine the scraped workpiece requires some pre-processing techniques to remove unwanted noises and enhance some important image features for further post-processing. Higher points on the scraped surface can then be identified. Tsutsumi et al. developed an image system with a CCD camera and a color filter that could recognize the higher points [2]. Yoshimi et al. recognized the higher points by a CCD line sensor and removed them by a grinder [3]. Such image processing, which offers a quick way to assess the quality of scraped surfaces, is useful for developing an automatic scraping machine [4]. In order to improve the quality of the scraping process, Tsutsumi et al. further developed an automatic scraping machine [5]. Tadanori et al. investigated the sequence of scraping operations to establish a standard manufacturing flow [6]. All of these works focus on 2-D image inspection followed by re-scraping of the surface to improve the quality.

Modern DVD players are well developed and their pickup heads have good focusing characteristics. Many applications use these low-cost DVD pickup heads for measuring features such as profile [7–9,22], velocity [10], straightness [11], angle [12], and acceleration [13–15]. Although there are some commercially available sensors or measurement systems that can measure the 3-D profiles of microstructured surfaces (e.g., the laser triangulation sensor, laser confocal sensor, laser confocal microscope, etc.), their costs are high. Furthermore, there are no reports on their application to scraped surface measurements thus far.

In this report, a 2-D image vision system that can assess only two quality parameters of the scraped surface, namely PPI and POP, is first studied. Subsequently, a 3-D profile measurement system to measure scraped surfaces—consisting of a DVD pickup head, an image processing system, and an XY stage—is presented. This system is able to analyze five parameters—namely the PPI, POP, HOP (or DOS), surface flatness, and oil content. In order to verify the 3-D measurement results, a separate image processing system is also developed to measure the PPI and POP, not only for the entire surface but also for each local area. This system can ensure the evenness of scraped spots for a uniform bearing load and a uniform velocity when the slider moves across the guideway. Experiments show that the two measurement systems yield consistent results, in which the 3-D system reveals more information about the quality of the scraped surface. Details of the hardware

configuration and the software and the computations are described in the following sections.

2. Measurement of 2-D scraped surfaces by computer vision

2.1. Digital image processing

Digital image processing techniques have been widely used in pattern recognition for some time. Characteristic features can be identified through a series of operations, such as noise reduction [16], auto threshold selection [17], edge detection [18–20], and mathematical morphology [21]. A variety of applications can be implemented by the use of image processing techniques, such as defect inspection of PC boards [23,24] and powder metallurgy products [25]. In this study, the parameters PPI and POP of the scraped surface are examined by a computer vision technique. The image system consists of a common CMOS sensor with 640×480 pixels and 8-bit gray levels, a properly selected lens, and a PC. The sequence of image processing techniques for this purpose is shown in the flow diagram of Fig. 1.

This flowchart shows that in automatic optical inspection, the camera needs to be calibrated with a commercially available standard template at the first step. After calibration, we know the dimensions of each pixel and the correction of the lens distortion. The second step is to threshold the gradient magnitude of edge points in order to extract the high-point areas. The potential edges of these high-point areas need to be identified first. These are done by applying Canny's edge detection technique [18]. From our long-term experiments over almost 1 year, however, we found that the detected edge points could not be extracted very repeatedly. It could be due to the varied room lighting conditions. To solve this problem, after

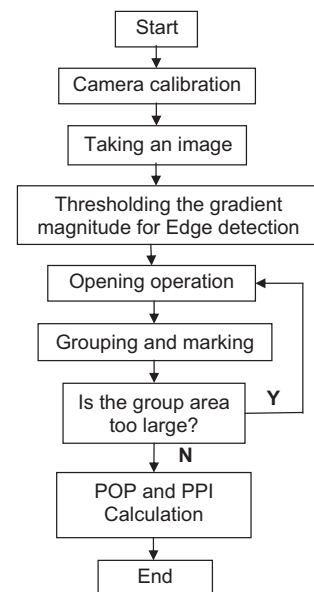


Fig. 1. Flow diagram of image processing.

the Canny's edge detection, we then adopted Sobel operators to mask all potential edge pixels to find the gradients (G_x and G_y) of each pixel's gray level in the X and Y directions, respectively. The magnitude of the gradient at each pixel is the vector sum of these gradients, i.e. $\nabla f = (G_x^2 + G_y^2)^{1/2}$. For all potential edge pixels in the image plane, a large gradient magnitude indicates a potential edge point as the gray level changes rapidly at this pixel point. A suitable ∇f value (t) is then selected as the threshold value to identify the edge points of high-point areas. For any pixel i , when its ∇f is higher than t its gray level is set to zero (black, which indicates a high point) and vice versa. The binarization function can be expressed by Eq. (1), where g_i is the original gray level, t is the threshold of ∇f , and $H(g_i)$ is the binarized gray level of each pixel.

$$H(g_i) = \begin{cases} 0 & \nabla f_i \geq t \\ 255 & \nabla f_i < t \end{cases} \quad (1)$$

After thresholding the gradient magnitude for edge detection, the high points can be identified. The next step is to apply a morphological opening operation to remove the noise of the binary image. Then, an 8-connected operation is used to group and mark connected high points, find the area of the group, and mark its centroid. The distribution of contact areas (high-point groups) in the image plane can be realized. It is noted that these contact areas are recognized by the tinted paste that generates low gray levels in the captured image. The paste, however, may cover a portion of the surrounding area of each high-point group and connect vicinal groups. This yields an excessively large contact area. An iterative process of opening and grouping is carried out to separate connected high points into individual sub-groups. Based on the expert rules of the scraping technique, the threshold of the high-point contact area is set to 500 pixels in our computer program. Finally, the last step is to calculate the following parameters: number of high points per area of square inch (PPI) and the percentage of points (POP).

This algorithm is validated by a number of computer generated scraped patterns. Fig. 2 is an example of a generated scraping pattern. Each high-point area is shown in black and its central point is recorded by a white dot. The areas of peak and valley zones can clearly be separated. In addition, as the size of the surface varies from case

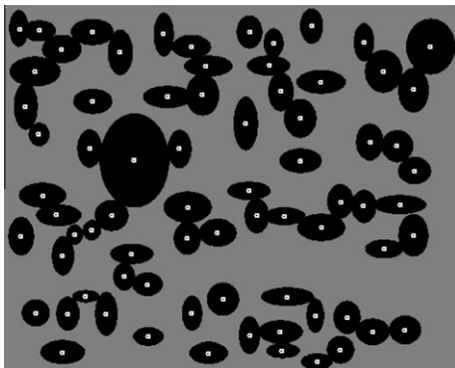


Fig. 2. Computer-generated pattern for testing.

to case, a better scraped surface should have evenly distributed patterns for the sake of a constant friction on the entire surface, although definitions of the PPI and POP refer only to the averaged values for the entire surface. Therefore, a moving window corresponding to a surface area of one square inch is generated. In the program, this window is automatically swept across the full image area in zig-zag motion with a feed size of one pixel. At each position, the parameters of PPI and POP are calculated. This is to assure that in addition to the full area, each local area is also evaluated. Although expert rules indicate that the best-scraped condition should have a PPI of 40 points and a POP of 50%, in practice, due to the manufacturing cost concern in industry acceptable ranges for the PPI and POP are between 20–25 points and 40–60%, respectively [1].

2.2. Experimental tests

A piece of a scraped surface made by a skilled craftsman is shown in Fig. 3. The picture on the left is the original image and the one on the right is the image after processing. The centroid marking of each black zone represents a peak area. In practice, the conventional tinted paste coating process is used to enhance the image contrast of the high points with respect to the low points. The results of five repeatability tests on the full area are shown in Table 1. The variation of PPI is 2.3 points and that of POP is 2%, which demonstrates that the 2D image processing method is highly replicable. The pictures also reveal that the spot distribution is uneven. The use of a moving window to evaluate local parameters is deemed necessary for the sake of a constant friction force along the full stroke sliding distance. Fig. 4 shows another example evaluated by a moving window. It shows that five local areas do not satisfy the expert rules, as marked by the square windows in the figure. Their actual positions are indicated by the (X, Y) coordinates of their respective upper left corners, and the types of no-go (NG) parameters are remarked in the last column of Table 2. It is seen that all five local regions fail to meet the required POP range (40–60%), being either lower (windows 1, 2, 3, and 5) or slightly higher (window 4). In addition, windows 1 and 5 require slightly more high points to meet the requirement (20–25 points). Note that although the averaged PPI and POP of the entire surface could be acceptable according to [1], these local unacceptable areas may cause velocity variation due to uneven friction forces when the carriage moves across these areas. This system provides a stricter rule than human justification. In practice, however, a slightly out-of-rules area such as window 4 could be regarded acceptable.

3. Measurement of a scraped 3-D surface by the focus probe

3.1. The focus probe module

Fig. 5 shows the optical system of a commercial DVD pickup head. The laser diode emits a beam through the grating. The beam then splits into three beams that pass

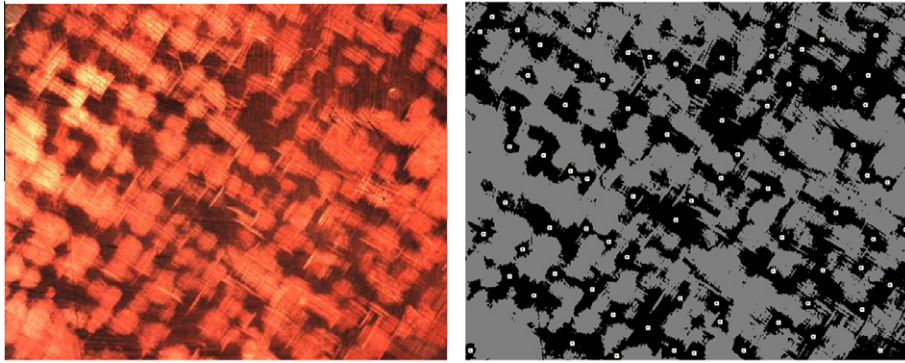


Fig. 3. Images of a scraped surface: (left) original and (right) after image processing.

Table 1

Repeatability tests for PPI and POP.

No.	PPI	POP (%)
Test 1	23.8	43
Test 2	24.4	41
Test 3	22.1	43
Test 4	23.6	43
Test 5	22.9	43

Table 2

Unacceptable local areas (NG means no go).

Window	X	Y	POP	PPI	Status
1	0	0	34.3	19	NG (POP and PPI)
2	390	0	30.8	24	NG (POP)
3	780	0	36.8	25	NG (POP)
4	1170	780	61.3	23	NG (POP)
5	0	1030	32.9	17	NG (POP and PPI)

through the polarization beam splitter, the quarter wavelength plate, the collimator lens, and the objective lens, and finally focus onto the disc surface. The reflected beam passes through the same original path, and after two polarizations by the quarter wavelength plate, projects onto the quadrant detector through the cylindrical lens. The photodiode outputs focus error signals (FESs) based on the astigmatic principle. If the measurement surface is near to or far away from the focal point, the image of the beam on the

photodiode becomes elliptically shaped in different orientations (Fig. 6, planes 1 and 3). If the measured surface is in focus, the image becomes circular (Fig. 6, plane 2). According to the beam spot distribution among the four quadrants, the FESs are used to measure the profile of the disc after calibration. A voice coil motor is used to trace the flight height change of the rotating disc. This focus or auto-focus probe technique has been developed over the course of more than 10 years by the author's group [8,9].

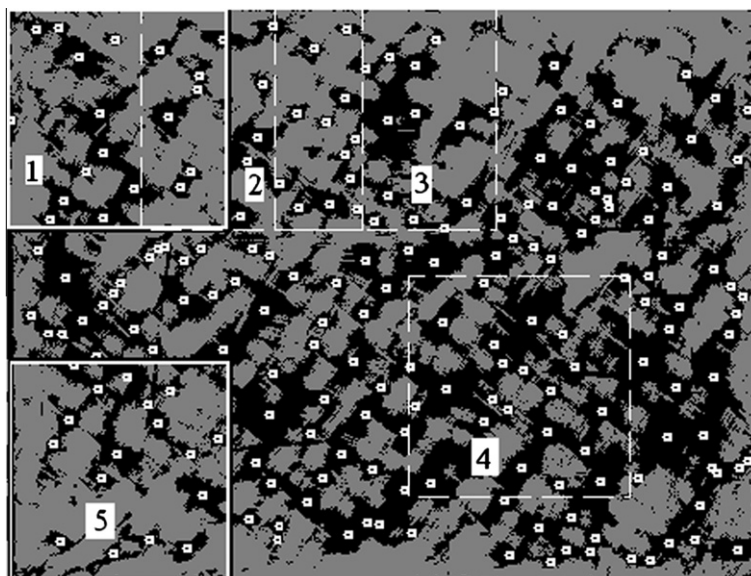


Fig. 4. Local quality evaluation by a moving window.

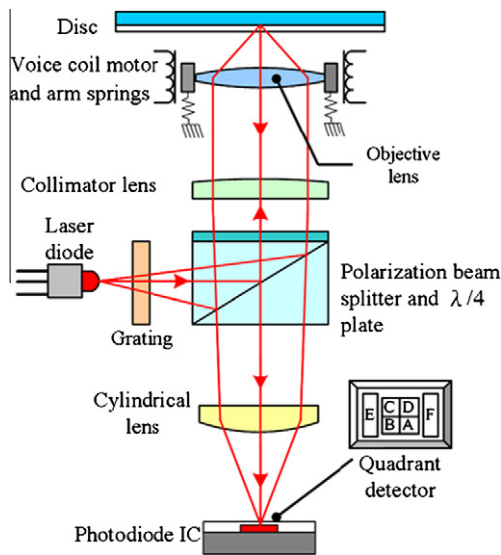


Fig. 5. Components of a DVD-pickup head.

The FES is processed by a differential circuit. Its linearity range is about 7 μm for a DVD and 20 μm for a CD, corresponding to numerical aperture (NA) of the pickup's objective lens (0.65).

The structure of the developed probe system is shown in Fig. 7. The original objective lens and voice coil motor of the DVD pickup head (Hitachi HOP-1000) are removed. A new microscope objective lens from NIKON (20×, NA 0.4) is mounted in order to increase the linearity range of the FES to about 20 μm. A CMOS camera can assist the user in viewing the exact measured point on the surface. Fig. 8 is a photo of the probe system with each component corresponding to the position in Fig. 7. For the sake of clarity, only some key components are labeled in this figure.

Given the surface reflectivity, the laser intensity on the photodiode is changed by the material comprising the

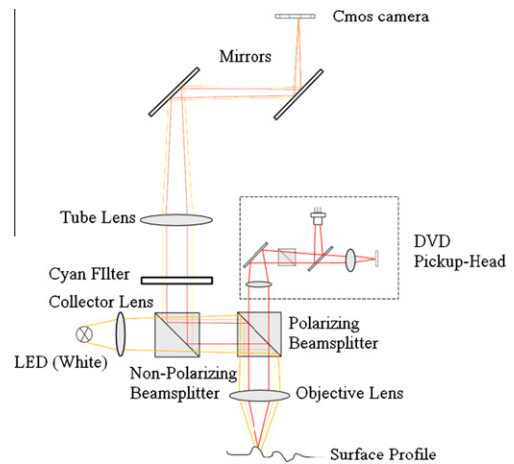


Fig. 7. Optical system of the developed focus probe.

object. The FES can be expressed by Eq. (2), where k is the reflection coefficient.

$$FES = k[(B + D) - (A + C)] \quad (2)$$

In order to eliminate the reflectivity effect, a normalization method is applied. This is achieved by dividing the FES by the sum of all intensities to yield what is called the normalized FES (NFES). The sum of the intensities is expressed by Eq. (3), and the NFES can be expressed by Eq. (4). It can be seen that the reflectivity no longer influences the NFES curve. This makes it possible to measure a surface with different reflection coefficients or using different materials with only one NFES curve. In practice, the scraped surface may have different reflection coefficients due to changes in color.

$$SUM = k(A + B + C + D) \quad (3)$$

$$NFES = FES/SUM = [(B + D) - (A + C)] / (A + B + C + D) \quad (4)$$

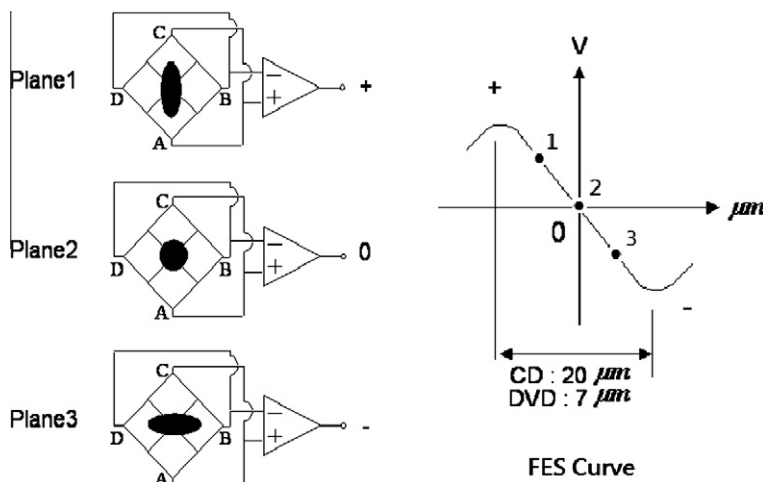


Fig. 6. Spot shape within the FES range.

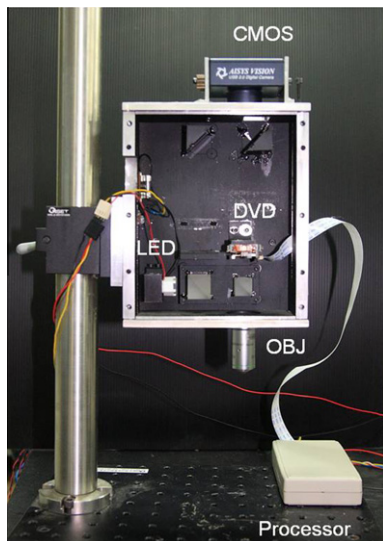


Fig. 8. Photo of the focus probe system.

3.2. Experimental setup and calibration

Fig. 9 illustrates the experimental setup. The entire scraped profile can rapidly be scanned by driving the motorized XY stage in zig-zag steps. The auto power control (APC) circuit provides the constant output power of the laser diode. The XY stage is controlled by two step motors with a microprocessor (AVR). The scanning speed is controlled to about 20 mm/s.

The scraped surface needs to be perfectly leveled to keep the entire surface profile within the linear range of the NFES. This system is calibrated by a laser interferometer (SIOS Co., SP-2000) on a ground surface of the same scraping material. The linearity range is about $18\ \mu\text{m}$ and the average error is about $0.3\ \mu\text{m}$, as shown in Fig. 10. From the expert rules [1], the peak-to-valley height of an accepted surface should be around $10\ \mu\text{m}$. This is just within the linear range of the NFES.

The profile of a measured scraped line by the developed focus probe system is compared with that of a commercial

profilometer (Talysurf PGI 1240, Taylor Hobson Co.). During the experiment, we attempted to match the lines as closely as possible. Given that this experiment dealt only with one line data, the above-mentioned image processing techniques could not be applied. We only used the simple moving average operation to filter out the noise of each measured data point. Comparison results are shown in Fig. 11a under the condition of setting both initial points to zero. The trends of the line profile are in good agreement. The magnitude of the profilometer measurement is on average higher than that of the focus probe measurement, especially at the peaks. When the slope is steep, the relative error becomes large. This could be caused by one or more of the following factors: (1) a slight offset in the compared lines when measured by two separate instruments; (2) the difference of stylus tips (diameter: $4\text{-}\mu\text{m}$ contact type for PGI 1240 and $1.6\text{-}\mu\text{m}$ noncontact type for focus probe); and (3) a correction factor is not applied when measuring a steep surface as the focus probe is calibrated by the height changes of a flat surface. From the error plot of Fig. 11b, the average difference is within $\pm 2\ \mu\text{m}$, except at a few highly sloped points. The profiler trend is reasonable; hence, it should not cause much deviation of the evaluated 2-D parameters (PPI and POP) and flatness, although it might affect the amounts of evaluated HOP (DOS) and oil retention volume to some degree. The focus probe system, however, is much cheaper, faster, and portable for use in the factory.

3.3. Parameter evaluation methods

The measured data contain noise, particularly at the sharp edge of each spot created by the scraper, as seen in Fig. 12a. At each position (x_i, y_i) there is a corresponding height (z_i) . A general 3×3 low-pass mask for image processing is used to convolute each point in order to remove this high-frequency noise. A clear 3-D topography of a scraped surface can then be used for data analysis, as shown in Fig. 12b. The measured 3-D profile can reveal more information on the surface characteristics. Given that the parameters related to the quality of a 3-D scraped surface have never been evaluated before, this report proposes the first evaluation methods for the following parameters.

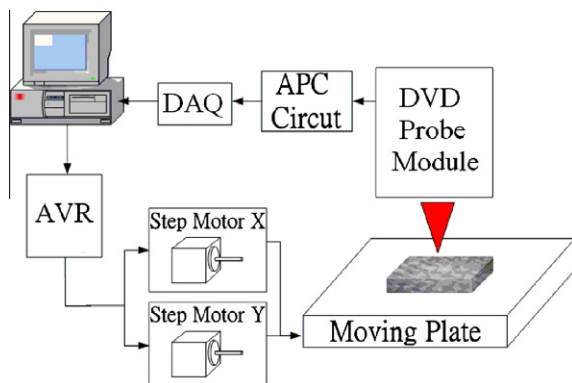


Fig. 9. Experimental setup of 3-D scraped surface measurement.

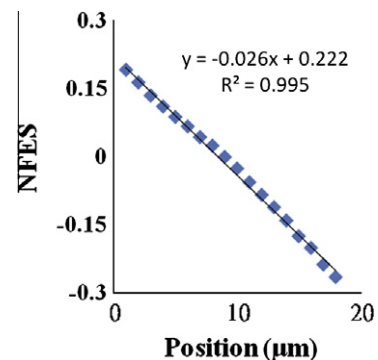


Fig. 10. Linear range of the normalized FES.

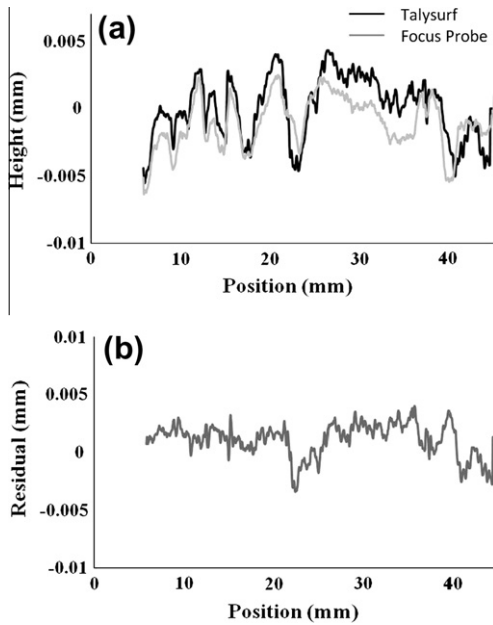


Fig. 11. (a) Comparison of a line measured with the focus probe or the Talysurf profilometer and (b) a plot of the difference.

3.3.1. Evaluation of PPI and POP

On a 3-D plot, the method of evaluating PPI and POP is similar to that of 2-D image processing. The height distribution across the entire surface is normalized to the range of 0–255, and the corresponding gray level is assigned to each point. Image processing techniques similar to those applied to the 2-D image in Section 2.1 are then applied to the gray-level image of these 3-D data. Fig. 13 shows the processed images measured by a CCD camera and the focus probe on the same sample. Both have identical POPs of 50%. The PPI for the camera image is 21.1 and that for focus probe image is 22.3. The absence of tinted paste coating during the focus probe measurement yields lower contrast for the entire image. Nonetheless, the evaluated results are almost the same.

3.3.2. Evaluation of HOP (or DOS)

From the smoothed 3-D topography (e.g., Fig. 12b) and its PPI calculation, the threshold separating the high-point areas from the surroundings can be obtained. The pro-

cessed image of Fig. 13b reveals the location of each high-point area. For the assessment of HOP (or DOS), the mean height of all peak zones and the mean depth of all valley zones are calculated. The distance in between is defined as the height of point (HOP) or the depth of the surrounding (DOS).

Let H_i indicate the mean height of the i th peak area ($i = 1$ to N) and D_j the mean height of the j th valley area ($j = 1$ to M). Then the formula for HOP (or DOS) can be expressed by

$$\text{HOP} = \left(\sum_{i=1}^N H_i \right) / N - \left(\sum_{j=1}^M D_j \right) / M \quad (5)$$

3.3.3. Evaluation of flatness and oil-retention volume

The surface flatness refers only to the bearing area that will be in sliding contact with the moving carriage. The contact areas have been separated from the surroundings by the threshold value during the image processing process. The average height of all threshold points (i.e., edge points) is defined as the threshold plane of the 3-D topography, as shown in Fig. 14. This threshold plane only provides a reference height. For each high-point area its central height relative to this threshold plane is recorded. Then, a least-squares (LSQ) plane passing through all central heights can be calculated. The peak-to-valley distance of the residuals referenced to the LSQ plane is defined as the flatness error of the bearing area. This approach is similar to the normal LSQ flatness analysis of any surface plate, with the exception that only the heights of all central points of contact areas are considered.

For the evaluation of oil retention volume, we assume the lubrication oil is filled full in all cavities of the scraped pattern. The LSQ plane expressed above represents the best-fit plane passing through all central points of the contact areas. Therefore, the amount of oil-retention volume can be defined as the sum of all volumes below this LSQ plane, as shown the shaded part in Fig. 14. Given that the measured data are digital, we can easily calculate this volume by summation of all heights below the LSQ plane in the computer program.

3.4. Experiments

Three sample plates were ordered from different scraping experts who work for different machine tool companies, to be scraped to the finest quality. Their photos are

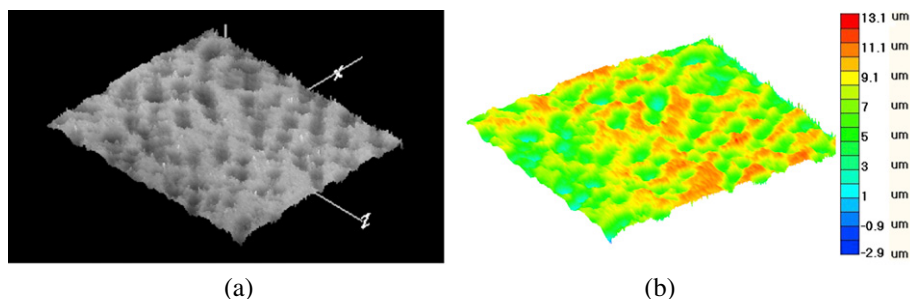


Fig. 12. Measured 3-D microstructure profile: (a) raw data plot and (b) smoothed data plot.

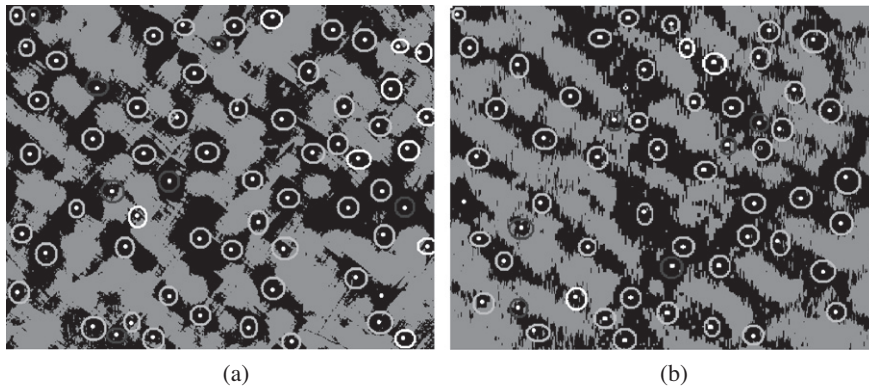


Fig. 13. Evaluation of PPI and POP: (a) measured by 2-D CCD camera and (b) measured by 3-D focus probe.

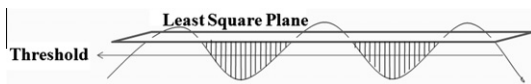


Fig. 14. Calculation of flatness and oil retention volume.

shown in Fig. 15a. Plates 1 and 2 were scraped to a similar pattern that is used for the slideway of a turning or milling machine. Plate 3, scraped to a different pattern, is used for

the Z-axis slideway of a grinding machine. Their 2-D image processing results are shown in Fig. 15b and their 3-D measurement results are plotted in Fig. 15c. Plate 1 was presented in Fig. 13 and its 3-D topography is the same as that shown in Fig. 12b. Five parameters are evaluated and listed in Table 3. It can be seen that although plates 1 and 2 are similar in their evaluated parameters, plate 1 shows larger flatness error. It can be predicted that the sliding contact performance of plate 1 will be worse. If

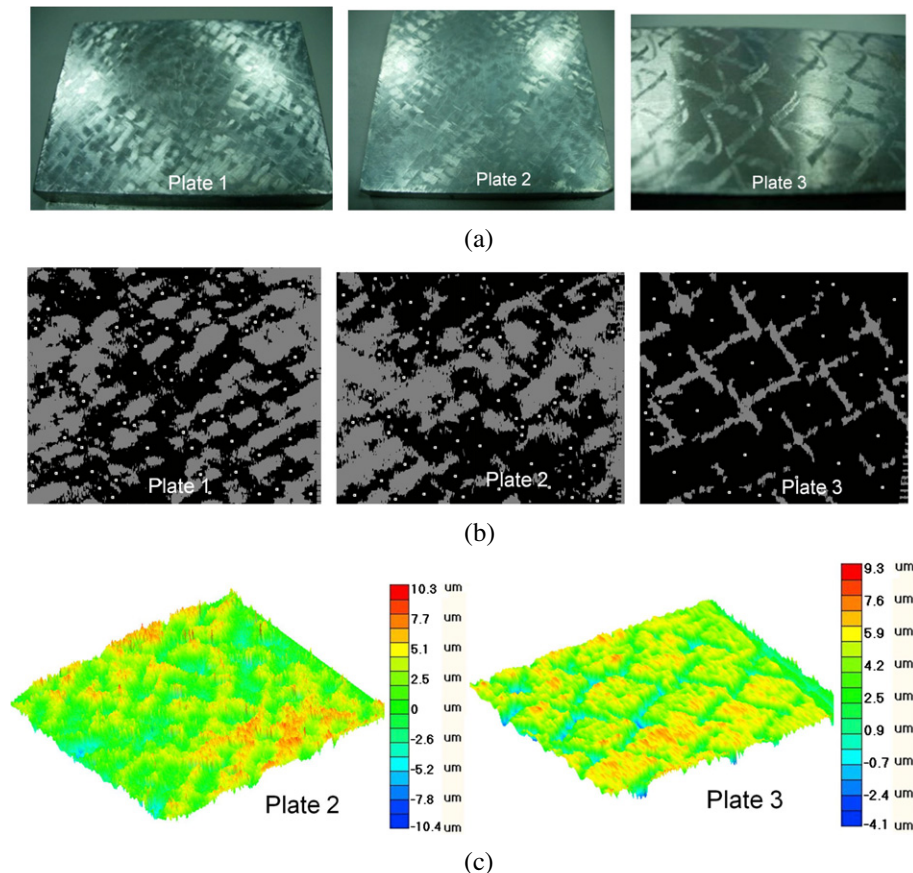


Fig. 15. Three scraped plates: (a) photographs, (b) corresponding 2-D image processing patterns, and (c) corresponding 3-D topography plots.

Table 3

Evaluated parameters for the three scraped surfaces.

Parameters	Plate 1	Plate 2	Plate 3
Total area (in. ²)	3.442	3.508	1.81
Total high points	72	67	30
PPI	20.9	19	16.5
POP (%)	54	56	83
HOP (DOS) (μm)	10.2	8.9	11.5
Flatness (μm)	4.5	3.9	1.5
Oil retention volume (cc)	0.00169	0.00229	0.00073

the local quality evaluation rule indicated in Section 2.2 and Fig. 4 is used, this plate needs to be re-scraped. Plate 3 is particularly scraped for the slideway in the Z-axis motion of the grinding machine. The grinding head as well as the grinding wheel has to remain good straightness during up and down motion along the machine tool column. In order to resist the grinding force, its bearing area ratio and flatness are of greatest concern. Although this plate does not fulfill the expert rules values, the manufacturer, however, requires more POP and better flatness for the acceptable quality of this work. From this investigation, it can be realized that with 3-D inspection and evaluation methods, more unknown phenomena of surface scraping techniques can be discovered.

4. Conclusions

In this report, we have proposed two investigation methods to evaluate the quality parameters of scraped surfaces. Although the 2-D image processing method is similar to other published methods in terms of hardware, the proposed method of local quality evaluation by a moving window throughout the entire image can help identify uneven distributions of scraped spots. Although it is not mentioned in the expert rules, a re-scraping process is therefore necessary. The current industrial evaluation technique can only quantify two parameters based on visual inspection, namely the PPI and POP. The more advanced 3-D measurement method based on the proposed focus probe system can significantly realize more parameters, including PPI, POP, HOP (DOS), flatness, and oil retention volume at the current time. Given that this 3-D method is the first of its kind, new evaluation methods for these parameters are proposed. Experimental results show the consistency of the proposed 2-D and 3-D systems, and suggest that more physical phenomena related to the quality and function of the scraped surface can be discovered with the latter. This is our first report on this subject. Further investigations to improve the evaluation and performance of the scraped surfaces from a 3-D view will be carried out in the future.

References

- [1] R. King, Scraping Technique Training Notes, King-Way Machine Consultants, Inc., Taiwan, 2008.
- [2] H. Tsutsumi, R. Yamada, A. Kyusojin, T. Nakamura, Development of an automatic scraping machine with recognition for bearing of

- scraped surfaces – recognition of black bearing by CCD camera (1st report), Journal of the Japan Society for Precision Engineering 62 (1996) 219–223.
- [3] T. Yoshimi, S. Masafumi, Y. Tetsuya, C. Masahiro, The recognition of bearings by means of a CCD line sensor and the automation of scraping works, NII-Electronic Library Service 71 (1986) 93–98.
- [4] H. Tsutsumi, R. Yamada, A. Kyusojin, T. Nakamura, Development of an automatic scraping machine with recognition for bearing of scraped surfaces – construction of automatic scraping machine (3rd report), Journal of the Japan Society for Precision Engineering 71 (2005) 358–362.
- [5] H. Tsutsumi, A. Kyusojin, T. Nakamura, Development of an automatic scraping machine with recognition for bearing of motion mechanism (2nd report), Journal of the Japan Society for Precision Engineering 62 (1996) 554–558.
- [6] S. Tadanori, Y. Yasuo, S. Itaru, N. Norihiko, Digitalization and intellectualization of scraping operation (1st report): investigation of a series of scraping operation by skillful worker, Journal of the Japan Society for Precision Engineering 69 (2003) 949–954.
- [7] J.H. Zhang, L.L. Cai, An autofocusing measurement system with a piezoelectric translator, Transactions IEEE-ASME on Mechatronics 2 (1997) 213–216.
- [8] K.C. Fan, C.Y. Lin, L.H. Shyu, The development of a low-cost focusing probe for profile measurement, Measurement Science and Technology 11 (2000) N1–N7.
- [9] K.C. Fan, C.L. Chu, J.I. Mou, Development of a low-cost autofocusing probe for profile measurement, Measurement Science and Technology 12 (2001) 2137–2146.
- [10] F. Quercioli, A. Mannoni, B. Tiribilli, Correlation optical velocimetry with a compact disk pickup, Applied Optics 36 (1997) 6372–6375.
- [11] K.C. Fan, C.L. Chu, J.L. Liao, J.I. Mou, Development of a high-precision straightness measuring system with DVD pick-up head, Measurement Science and Technology 14 (2003) 47–54.
- [12] T.R. Armstrong, M.P. Fitzgerald, An autocollimator based on the laser head of a compact-disk player, Measurement Science and Technology 3 (1992) 1072–1076.
- [13] C.L. Chu, C.H. Lin, Development of an optical accelerometer with a DVD pick-up head, Measurement Science and Technology 16 (2005) 2498–2502.
- [14] C.L. Chu, C.H. Lin, K.C. Fan, Two-dimensional optical accelerometer based on commercial DVD pick-up head, Measurement Science and Technology 18 (2007) 265–274.
- [15] Y.C. Liu, K.C. Fan, C.L. Chu, C.A. Werner, G. Jager, Development of an optical accelerometer for low-frequency vibration using the voice coil on a DVD pickup head, Measurement Science and Technology 19 (2008) 1–7.
- [16] W.Y. Wu, M.J. Wang, C.M. Liu, Performance evaluation of some noise reduction methods, CVGIP: Graph Models Image Process 54 (1992) 134–146.
- [17] N. Otsu, A threshold selection method from gray-level histograms, IEEE Transactions on Systems, Man and Cybernetics (SMC) 9 (1979) 62–66.
- [18] J. Canny, Computational approach to edge detection, IEEE Transactions on Systems, Man and Cybernetics PAMI 8 (1986) 679–698.
- [19] J.H. Elder, S.W. Zucker, Local scale control for edge detection and blur estimation, IEEE Transactions on Pattern Analysis and Machine Intelligence 20 (1998) 699–716.
- [20] D. Marr, T. Poggio, Theory of edge detection, Proceedings of Royal Society, London B207 (1980) 187–217.
- [21] R.M. Haralick, S.R. Sternberg, X.H. Zhuang, Image analysis using mathematical morphology, IEEE Transactions on Pattern Analysis and Machine Intelligence 5 (1983) 532–550.
- [22] N. Islam, R. Parkin, P. Mueller, M. Jackson, K.C. Fan, Surface profile measurement system for timber, in: Proceedings of the 17th International DAAAM Symposium, Vienna, Austria, November 08–11, 2006, pp. 175–176.
- [23] Y. Hara, N. Akiyama, K. Karasaki, Automatic inspection system for printed-circuit boards, IEEE Transactions on Pattern Analysis and Machine Intelligence 5 (1983) 623–630.
- [24] G.A.W. West, A system for the automatic visual inspection of bare-printed circuit boards, IEEE Transactions on System Man and Cybernetics 4 (1984) 767–773.
- [25] K.C. Fan, J.Y. Chen, S.H. Chen, W.P. Liao, Development of auto defect classification system on porosity powder metallurgy products, NDT & E International 43 (2010) 451–460.